



## Inhibition of coagulation by macromolecular complexes

Keith Gomez  
John H. McVey  
Edward Tuddenham

The role of vertebrate blood coagulation is to rapidly prevent the loss of body fluids following vascular injury without compromising blood flow through either the uninjured or damaged vessels. To achieve this the coagulation network is initiated and regulated by a complex network of interactions that are under the control of both positive and negative feedback loops that result in controlled fibrin deposition and platelet activation only at the site of injury. Anticoagulant molecules play key roles in preventing inappropriate initiation of coagulation as well as down-regulating thrombin generation at the site of injury. Tissue factor pathway inhibitor (TFPI) inhibits the initiation complex, antithrombin (AT) inhibits the active serine proteases directly, whereas the activated protein C pathway inhibits coagulation by inactivating the cofactors V and VIII. In this review the structure and function of these anticoagulant molecules and their inhibitory complexes is discussed.

Key words: tissue factor pathway inhibitor, antithrombin, protein C, anticoagulation, serpin.

Haematologica 2005; 90:1570-1576

©2005 Ferrata Storti Foundation

From the MRC Clinical Sciences Centre, Imperial College London, Hammersmith Hospital Campus, London, UK.

Correspondence:  
Professor Edward G.D. Tuddenham,  
Haemostasis and Thrombosis  
MRC Clinical Sciences Centre  
Imperial College London,  
Hammersmith Hospital Campus  
Du Cane Road, London W12 0NN,  
UK. E-mail:  
edward.tuddenham@csc.mrc.ac.uk

The purpose of the coagulation network is to produce a focused burst of fibrin clot formation at the site of vascular injury (Figure 1). Not only does the process need to be rapid, it also needs to be tightly controlled to prevent the potentially disastrous consequences of clot dissemination through the intact vasculature. The original waterfall and cascade hypotheses of coagulation described a series of enzymatic reactions following each other sequentially.<sup>1,2</sup> In this model each zymogen is activated before acting on the next zymogen in the pathway in a series of discrete reactions. Although this explains the catalytic steps required in fibrin clot formation, it alone does not explain the kinetics of the process. It is now clear that, with certain exceptions, all of the reactions occur at the physiologically required rate only when the component molecules form complexes incorporating the substrate, enzyme and co-factor bound to negatively charged phospholipid. The exceptions are the procoagulant reactions catalysed by thrombin and the activation of factor (F) IX by FXIa. In the resting state phospholipid membranes are actively held such that the negatively charged phospholipids that provide the platform for these complexes are sequestered away from their outer surface. Following activation of cells such as platelets, the negatively charged phospholipids are *flipped* to the outer surface enabling the complexes to form more efficiently. Many pro-coagulant and anti-coagulant proteins have specialized N-terminal domains (G1a) containing post-translationally modified glutamic acid residues that mediate the phospholipid interaction. The incorporation of calcium ions in the G1a domain provides the necessary tertiary structure for this interaction to occur. The importance of this post-translation modification to appropriate blood coagulation is demonstrated by the action of warfarin which targets vitamin K epoxide reductase complex subunit 1.<sup>3</sup> The anticoagulant effect of this drug is due to the production of proteins with reduced  $\gamma$ -carboxylation of glutamic acid residues and hence decreased capacity to bind calcium. Once all the required components are assembled the substrate becomes activated by limited proteolysis and may then form a complex in which it is the enzyme with its own co-factors and substrates, thus producing a series of macromolecular complexes. Understanding how the complexes of FVIIIa-FIXa (the tenase complex) and FVa-FXa (the prothrombinase complex) are formed has been fundamental to our understanding of how coagulation proceeds *in vivo*.<sup>4</sup> At the same time that thrombin generation is leading to platelet activation and fibrin clot formation, negative feedback pathways and specific inhibitors are brought into play to regulate and terminate the process. Our current understanding of coagulation is based on

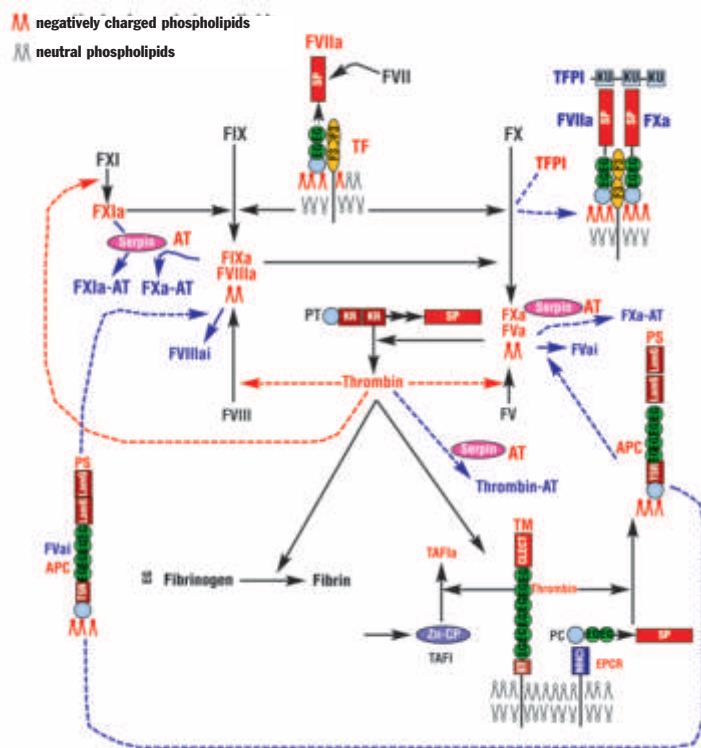


**Figure 1.** The inhibition of coagulation. The initiation of blood coagulation via generation of FIXa and FXa by TF-FVIIa is shut down by the action of TFPI, which forms a quaternary complex with TF-FVIIa-FXa. The serine proteases FIXa, FXa, FXIa and thrombin are all inhibited by antithrombin. Thrombin bound to thrombomodulin on endothelial cell surfaces activates protein C bound to its receptor, EPCR. APC in complex with its co-factor protein S inactivates FVa and in complex with FV/FVai inactivates FVIIIa by further proteolytic cleavages. Dashed blue arrows indicate negative feedback loops. The modular organization of proteins is indicated. Protein names are colored: functionally active proteins, red; inactive proteins black; inactivated or inhibited proteins, blue. All abbreviations are those explained in the text other than PS: protein S; PC: protein C; AT: antithrombin.

knowledge of the enzyme kinetics and demonstrations of the structural interactions between the components. Much of the information on the formation of the macromolecular complexes comes from X-ray and electron crystallography and nuclear magnetic resonance. Where this is not feasible computer modelling based on homologous structures has been used. The macromolecules involved in the initiation and amplification of the network have been discussed previously<sup>5</sup> and we now focus on those that regulate and/or terminate thrombin generation.

There are three major points in the coagulation network where inhibitory molecules act (Figure 1). These are: the inhibition of the initiating complex by tissue factor pathway inhibitor (TFPI); the inhibition of the serine proteases by serpin protease inhibitors (serpins), particularly anti-thrombin and the conversion of the co-factors FVIIIa and FVa to their inactive forms by the activated protein C (APC) pathway. In this short review we shall consider the interaction between the proteases and their major inhibitors at each of these points and the activation of protein C by thrombin, as these are the steps for which high quality structural information is available. All the 3D images depicted in this review were created from the PDB data files held at the Protein Data Bank (<http://www.rcsb.org/pdb/>)<sup>6</sup> using Accelrys Viewer Lite (<http://www.accelrys.com/>). As indicated above the complexes are dependent *in vivo* on the availability of a suitable negatively charged phospholipid surface and  $\text{Ca}^{2+}$  ions, which are not shown in the images.

### TFPI

The coagulation network is initiated by the binding of FVII/FVIIa to tissue factor (TF). The subsequent binding and activation of FX results in the formation of the trimolecular complex TF-FVIIa-FXa and an initial trickle of thrombin (FIIa) formation via direct activation of prothrombin (FII) by FXa in the absence of its co-factor FVa. Proteolytic activation of the zymogen coagulation proteases produces a neo N-terminus that is inserted into the catalytic domain, generating active serine proteases. Generally this class of enzyme is inhibited by serpins but it has been shown that serpins such as antithrombin inactivate the initiator complex too slowly to be relevant *in vivo* and that the main inhibitor of the initiator complex is TFPI.<sup>7</sup> This Kunitz-type inhibitor binds to form a quaternary complex that inhibits both FVIIa and FXa (Figure 2). It has been shown that inactivation of TF-FVIIa by TFPI is dependent on both calcium and FXa<sup>8</sup> indicating that TFPI only inhibits the complex after sufficient FX has been activated to allow thrombin to be generated. It does not, therefore, prevent coagulation from being initiated but rather limits further generation of FIXa and FXa by the TF-FVIIa complex. On account of the dependence on FXa, it is generally assumed that TFPI binds free FXa first and TF-FVIIa subsequently. However, there are kinetic data suggesting that TFPI can bind TF-FVIIa if FXa is in the near vicinity and thus it remains to be resolved which of these interactions occurs first *in vivo*.<sup>9</sup>

Circulating TFPI is bound by lipoproteins, in particular low-density lipoproteins, and there is close correla-

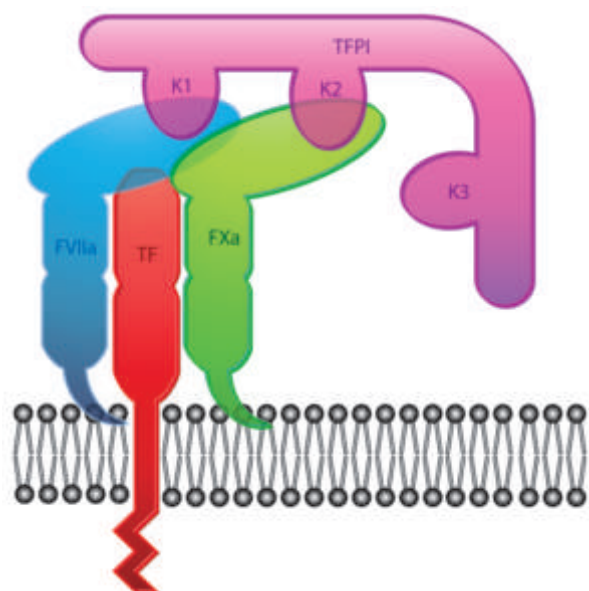


**Figure 2.** Inhibition of the initiating complex by tissue factor pathway inhibitor. Kunitz domains (K1 and K2) of TFPI bind with activated factor VII (FVIIa) and factor X (FXa). The third Kunitz domain (K3) and C-terminus of TFPI may interact with the plasma membrane.

tion between plasma levels of TFPI and low-density lipoproteins.<sup>10</sup> In the circulation TFPI is partially truncated by proteolysis such that there is a mixture of forms of variable length, ranging from full length to loss of the carboxy-terminus and sometimes part of the K3 domain. These shortened forms of the molecule have reduced inhibitory activity in comparison with full length TFPI.<sup>8</sup> TFPI bound to lipoprotein is inactive. The major pool of functionally active TFPI is found on the endothelial cell surface. The administration of heparin substantially increases plasma TFPI concentrations suggesting TFPI is in complex with glycosaminoglycans on the endothelial cell surface. The release of TFPI from the cell surface may partly explain the anticoagulant effect of this drug.<sup>11</sup> Recent data suggest that a further large pool of TFPI is associated with a glycosyl-phosphatidylinositol (GPI) linked protein on the surface of endothelial cells. Furthermore, there is also a pool of TFPI contained in the  $\alpha$ -granules of platelets which is released upon platelet activation.

After its formation on the cell surface, the quaternary complex (TF-FVIIa-FXa-TFPI) interacts with cell surface receptors such as the low-density lipoprotein receptor-related protein possibly through the C-terminus of TFPI. This leads to endocytosis of the complex, degradation and ultimately down-regulation of TF expression.<sup>12,13</sup> Other cell surface receptors may also be involved in this process as there is good evidence that endocytosis can occur independently of the low-density lipoprotein receptor-related protein.<sup>14,15</sup> There is increasing evidence that in addition to its role in fibrin

clot generation the initiating complex activates cell signaling pathways by cleavage of protease activated receptors. The physiological importance of this function remains unclear but inhibition by TFPI effectively silences the TF-FVIIa cell signaling pathway. Interestingly in a Chinese hamster ovary cell model system recombinant TFPI had little effect on cell signaling pathways at concentrations that effectively inhibited FXa generation.<sup>16</sup> These results suggest a critical role for proper positioning of TFPI on the cell surface, through association with glycosaminoglycans or glycosyl-phosphatidylinositol-anchored protein(s), for efficient inhibition of TF-VIIa cell signaling.

The domain structure of TFPI is typical of inhibitors acting on multiple similar proteases in that it consists of a series of homologous regions with crucial subtle differences that determine substrate specificity. The homologous regions are three Kunitz-type domains (K1-3) followed by a long carboxy-terminus. The protease inhibitory function resides in the Kunitz domains with K1 interacting with FVIIa and K2 with FXa. The functions of the K3 domain and carboxy-terminus remain to be fully elucidated. As there is no evidence of a direct interaction between the K3 domain or carboxy-terminus and FVIIa or FXa, these regions may be involved in stabilizing the final complex on the cell surface.<sup>17</sup>

The crystal structure of the quaternary complex FVIIa-TF-FXa-TFPI is not yet available but the interface between these molecules can be inferred from the known structures of TFPI Kunitz domains in isolation and in complex with trypsin. From these structures it seems that the critical segment in the Kunitz domains that are involved in protease binding involves residues 10-20 (boxed residues Figure 3). Numbering in this review follows the convention of using the numbers of the archetype for a protein family, in this case bovine pancreatic trypsin inhibitor.<sup>18,19</sup> This sequence forms the reactive center loop that interacts closely with the catalytic domain of the protease lying just below the catalytic groove in the quaternary complex (Figure 4). The residue at the center of the loop (Lys15 in K1 and Arg15 in K2) assumes particular importance and replacement with a non-basic side chain greatly reduces inhibitory potential.<sup>18</sup> The residue at position 15 corresponds to the P1 residue marking the position of the scissile bond that is cleaved in normal substrates. However, TFPI acts as a pseudo-substrate because the reactive center loop is a rigid structure that resists proteolysis. Once the reactive center loop is bound in the active site a stable complex is formed and the enzyme is blocked from further catalytic activity. An alignment of TFPI sequences across species demonstrates that the Kunitz domains are highly conserved in comparison with the remainder of the molecule (Figure 3). In particular this shows that the residue at the center of the reactive center loop is invariably an arginine or lysine. It can be seen that in

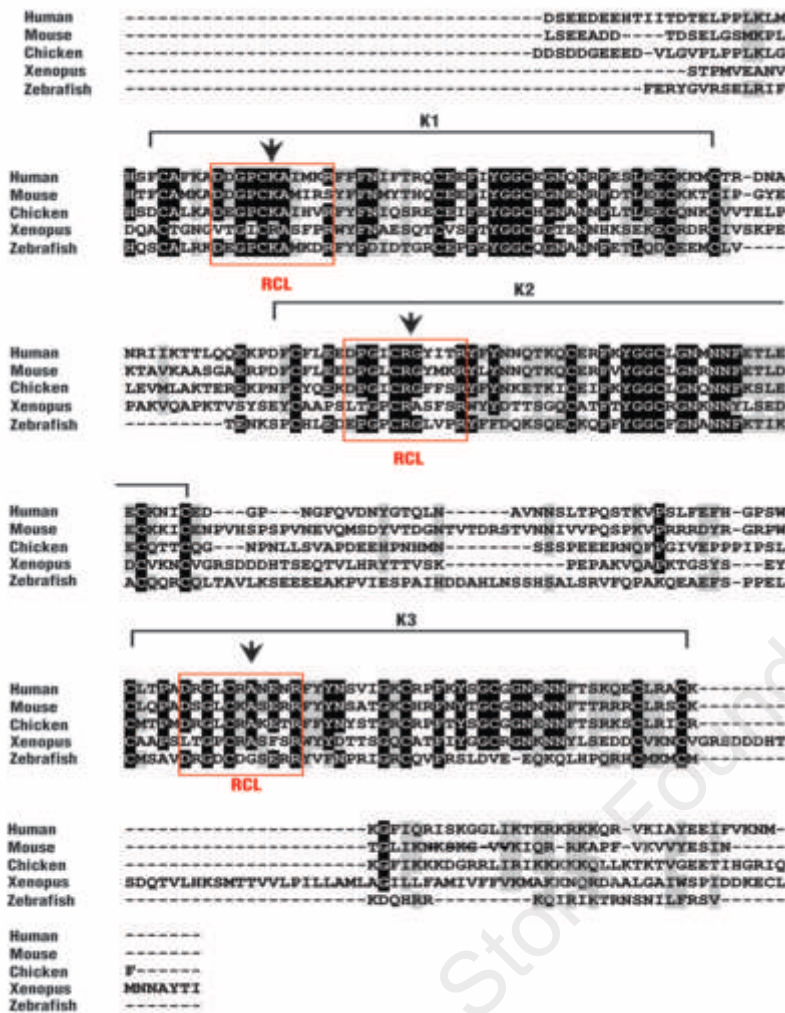


**Figure 3.** Sequence alignments of TFPI from various species. The sequences were aligned using ClustalW, following a Phi-blast search (<http://www.ncbi.nlm.nih.gov/BLAS>) with the human TFPI amino acid sequence to identify proteins with sequence identity. The figure was generated using Bioedit (<http://www.mbio.ncsu.edu/BioEdit/bioedit.html>). White on black indicates identity with the consensus; black on gray indicates similarity with the consensus. K1, Kunitz domain 1; K2, Kunitz domain 2; and K3, Kunitz domain 3. The black arrows indicate the residue in each Kunitz domain that would correspond to the P1 residue. The red box highlights the reactive center loop (RCL).

some species, including man, a basic residue is also found in the same position in K3 suggesting that this domain could have an inhibitory function, although at present there are no candidate enzymes for this domain.

### Antithrombin

After the trickle of thrombin production that results from the formation of the initiating complex and activation of prothrombin by FXa, subsequent thrombin generation speeds up exponentially once the co-factors V and VIII have been activated.<sup>20</sup> This is due to formation of the tenase complex FVIIIa-FIXa and the prothrombinase complex FVa-FXa. Although the basic tertiary structure of thrombin is similar to that of other members of its protease family (of which the archetype is chymotrypsin), it contains a number of unique loops. Some of these form anion-binding exosites that are involved in substrate recognition and allow thrombin to have a wide variety of substrates resulting in both procoagulant and anticoagulant functions. Exosite I is essentially procoagulant and is required for cleavage of substrates such as fibrinogen, while exosite II is antico-

agulant and binds heparin. In addition to its many functions in the coagulation network, thrombin also cleaves protease activated receptors, indicating that it may have important roles in cell signaling pathways.

Although there are various serpins that can inactivate thrombin, the most important in physiological terms is antithrombin. This inhibitor also has a physiological role in inactivating FXa and possibly also FIXa and FXIa (Figure 1). As with the other serine proteases the tertiary structure of the thrombin/antithrombin brings the catalytic triad of His57, Asp102 and Ser195 (chymotrypsin numbering) together at the bottom of the reactive site. Unlike the Kunitz-type inhibitors such as TFPI, antithrombin has a reactive center loop that is not held rigidly by disulfide bonds but is able to swing in a hinge-like manner. In the resting state the reactive center loop projects above the body of the serpin. When the reactive center loop docks with the thrombin reactive site the Arg393-Ser394 peptide bond in the center of the reactive center loop is cleaved (Figure 5). At this stage the complex is in a covalently linked intermediate form that is similar to those formed between thrombin and its procoagulant substrates. Normally a substrate

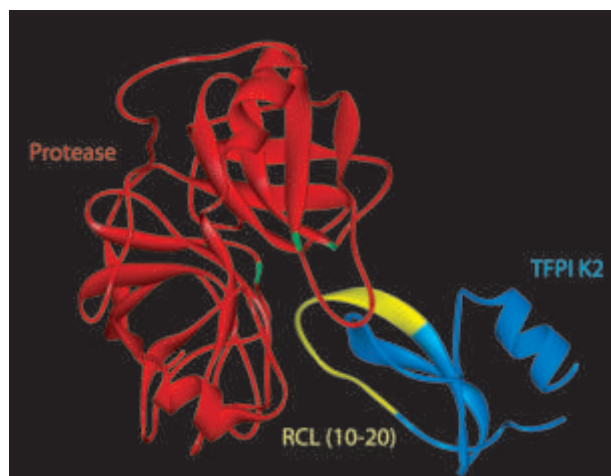


**Figure 4.** Ribbon model of the TFPI K2 and porcine trypsin complex. The reactive center loop of the Kunitz domain, incorporating residues 10-20, is in yellow with the protease catalytic triad of His57, Asp102 and Ser195 in green. PDB ID: 1TFX.

would dissociate after cleavage, thereby regenerating the active enzyme. In contrast, antithrombin remains linked to thrombin by one arm of the now cleaved reactive center loop such that the enzyme is effectively trapped. This arm becomes inserted into the body of the serpin as an additional  $\beta$ -pleated sheet with the protease swung to the bottom of the inhibitor.<sup>21,22</sup> This produces a stable complex in which the thrombin reactive site is squashed against the body of the inhibitor, distorting it and resulting in irreversible inhibition. The two loops of thrombin on either side of the reactive cleft, which form the 148 loop (also called the  $\gamma$ -loop) and 220 loop (which together with the 180 loop forms the  $\text{Na}^+$  binding site), are critical in determining specificity for antithrombin rather than other serpins. These two loops effectively prevent inhibitors such as bovine pancreatic trypsin inhibitor from docking with the reactive site but form important interactions with the main body of AT.<sup>23</sup>

Antithrombin by itself is a weak inhibitor of thrombin. The extensive interactions that are required between the two molecules do not take place easily without assistance. This may be because of repulsion between the highly charged surfaces of the two molecules.<sup>24</sup> The action of antithrombin is greatly enhanced by glycosaminoglycans such as the naturally occurring heparan sulfate or the various tissue-derived heparins that are widely used as anticoagulants in clinical practice. Antithrombin binds in a highly specific fashion to a unique pentasaccharide sequence in heparin. This induces a conformational change in the reactive center loop that is alone sufficient to enhance inhibition of FXa. This understanding has led to the development of synthetic molecules containing the pentasaccharide sequence which are useful in therapeutic anticoagulation. Binding of the pentasaccharide sequence to



**Figure 5.** Ribbon models showing inhibition of a serine protease by a serpin. On the left the serpin ( $\alpha$ 1-antitrypsin in blue) has aligned with its target protease (trypsin in red, with catalytic triad residues in green). The serpin reactive center loop (RCL) inserts into the reactive site and is cleaved between Met358-Ser359 as described in the text. On the right part of the cleaved RCL has been inserted as an additional sheet into the main part of the serpin. The protease remains linked to Met358 and is swung down and pressed against the body of the serpin. PDB IDs: 1H4W, 1QLP and 1EZK.

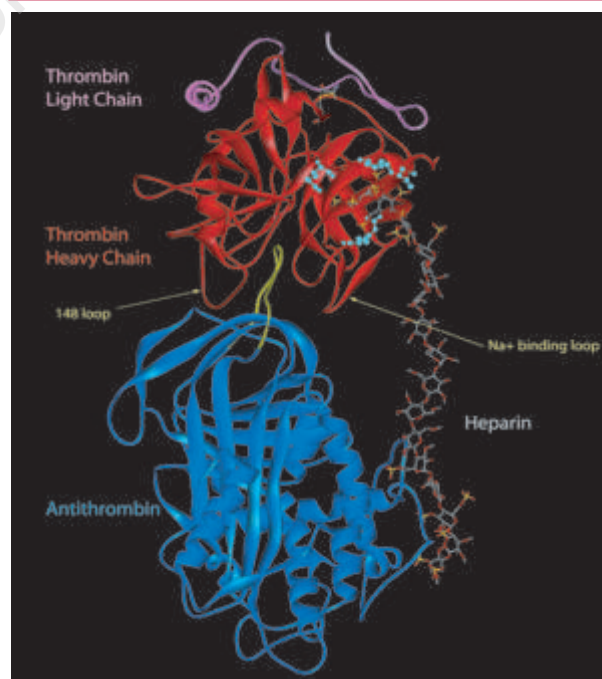


**Figure 6.** Ribbon model of the thrombin-antithrombin-heparin complex. Antithrombin is in blue, thrombin heavy chain in red and light chain in pink with the disulfide bond Cys1-Cys122 shown as a line model and heparin as a line model. The reactive center loop (RCL) of antithrombin is shown in yellow. R93, R233, K236 and K240 (cyan ball and stick models) in thrombin exosite II bind to heparin and the 148 and  $\text{Na}^+$  binding loops interact with the body of antithrombin. PDB ID 1TB6.

antithrombin does not, however, lead to full enhancement of thrombin inhibition. This requires subsequent binding of thrombin to heparin, with recognition of an oligosaccharide of variable length in heparin by a number of basic arginine and lysine residues that together form exosite II in thrombin.<sup>25</sup> The sequence of events seems to be that antithrombin binds to heparin via the highly specific pentasaccharide and thrombin binds distal to this region and then moves along the heparin molecule until it encounters the inhibitor. This leads to further conformational changes that orientate the reactive center loop with the thrombin reactive site and importantly forces antithrombin and thrombin into the close proximity required for full inactivation (Figure 6). Once the tri-molecular complex has been formed, inhibition is completed by the mechanism described above and heparin can dissociate and interact with further free antithrombin. The antithrombin-thrombin complex that remains is stable and irreversible.

### Protein C pathway

While antithrombin effectively inhibits the procoagulant effect of thrombin and leads to its removal from the circulation there is a molecule that goes much further. The binding of thrombin to thrombomodulin modifies a number of its functions, effectively switching them from procoagulant to anticoagulant activities. The main functions of the FIIa-thrombomodulin complex are the activation of the anticoagulant protein C and the anti-fibrinolytic thrombin-activatable fibrinolysis inhibitor (TAFI) (Figure 1).<sup>26,27</sup>

Thrombomodulin is a trans-membrane protein containing a serine-threonine rich domain adjacent to the membrane, followed by six epidermal growth factor (EGF)-like domains and a lectin-like globular domain. The central portion of the molecule, EGF4-6, is primarily responsible for binding thrombin and providing the co-factor function that leads to protein C activation. As can be seen in Figure 7, EGF5-6 of thrombomodulin and the anion binding exosite I of thrombin interact via a series of hydrogen bonds across their hydrophobic surfaces.<sup>28</sup> It is apparent from this view that EGF5 is folded in a manner that is not typical of EGF domains in other proteins. The tertiary structure of EGF domains is dependent on disulfide bond formation between pairs of cysteine residues within the domain. In EGF4 and EGF6 of thrombomodulin the cysteines are paired 1-3, 2-4 and 5-6 as in most other proteins and thus a typical tertiary structure is formed. In EGF5 the cysteines are paired 1-2, 3-4 and 5-6 resulting in an unusual folding with extension of the major  $\beta$ -sheet. The folding of EGF5 in this manner points EGF4 away from the interaction with thrombin exosite I. As EGF4 does not interact directly with thrombin, but is nevertheless essential for activation of protein C, it has been postulated that it binds protein C allowing optimal alignment of the

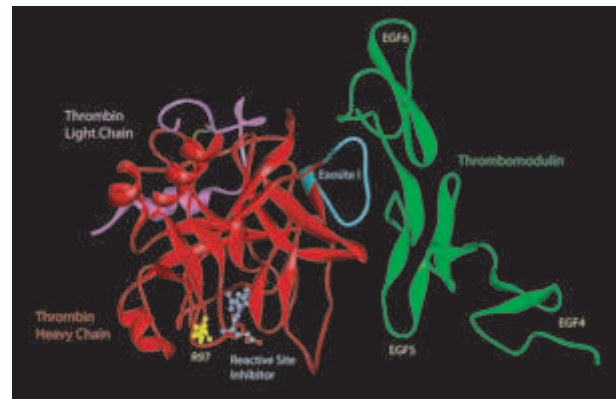


**Figure 7.** Ribbon model showing thrombin complexed with a thrombomodulin fragment. The image is oriented such that the membrane would be at the top of the figure. The thrombomodulin fragment is in green with thrombin marked as in the previous figure. The thrombin inhibitor EGR-CMK is shown as a ball and stick model in the reactive site. EGF5-6 of thrombomodulin interacts with thrombin via exosite I (cyan residues). R97, which critically interacts with chondroitin sulphate, is shown as a yellow ball and stick. The long axis of EGF4 points away from thrombin. PDB ID 1DX5.

protein C activation peptide with the thrombin active site.<sup>26,28</sup> The FIIa-thrombomodulin complex is further stabilized by a chondroitin sulfate moiety that is O-linked to the serine-threonine-rich domain of thrombomodulin and extends away from the membrane towards thrombin, interacting with basic residues in exosite II. The most critical of these is Arg97 (yellow ball and stick in Figure 7), which sits adjacent to the reactive site. Mutating this residue to the non-basic Ala prevents chondroitin sulfate-dependent inhibition of thrombin without affecting the ability of the FIIa-thrombomodulin complex to activate protein C.<sup>29</sup> The binding of thrombomodulin EGF5-6 to exosite I prevents this region of thrombin from binding to procoagulant substrates and in addition leads to allosteric changes in the reactive site that enable cleavage of protein C. The domain structure of protein C is the same as that of the serine proteases of coagulation (FX, FIX and FVII) with a calcium containing Gla domain that is important in binding to phospholipids. In contrast with the other (procoagulant) serine proteases, protein C has a specific receptor: the endothelial protein C receptor (EPCR), which it binds to via its Gla domain.<sup>30</sup> Antibodies to EPCR can be found in disease states and have been shown to inhibit the activation of protein C on the endothelium, indicating that it is the EPCR rather than membrane phospholipids that is important in protein C activation.<sup>31</sup> The requirement for a specific receptor for protein C may be due to the relatively low affinity of its Gla domain for negatively charged phospholipids in comparison with other vitamin K – dependent coagulation factors.<sup>32</sup> Additionally it may allow activated protein C (APC) to carry out a number of specific functions in other pathways. It is now well

established that the anticoagulant pathways discussed above have an important role in the regulation of inflammation and that thrombomodulin and APC appear to be most important in linking coagulation and inflammation.<sup>33</sup> The anti-inflammatory activities of thrombomodulin may depend principally on the lectin-like domain. Mice with a truncated thrombomodulin in which the lectin-like domain has been deleted have normal activation of protein C but an impairment of the anti-inflammatory properties of the endothelium such that they have reduced survival after exposure to endotoxin.<sup>34</sup> APC carries out its main anticoagulant functions of inactivating FVa and FVIIIa only after recruiting protein S as a co-factor. Neither full length protein S nor any of the protein S-containing complexes have been crystallized to date and our understanding of its involvement comes from theoretical models based on biochemical data and homologous structures. In the circulation 60% of protein S is inactive by virtue of being bound to C4b binding protein via two laminin

G-type domains at its N terminus.<sup>35</sup> The free active form interacts with negatively charged phospholipids via the C terminal Gla domain in a Ca<sup>2+</sup> dependent fashion. The Gla domain is followed by a region sensitive to cleavage by thrombin and FXa followed by four EGF domains. It is likely that the EGF domains mediate binding to APC. The APC-protein S complex is then able to effectively cleave membrane bound FVa.<sup>30</sup> The cleavage of FVIIIa is dependent on the presence of inactivated FV but does not seem to require protein S. Although our current understanding is that protein S has its anticoagulant effect through APC there is some interesting evidence that it can inhibit the tenase and prothrombinase complexes directly *in vitro*.<sup>35</sup> Whether this direct inhibitory effect is physiologically significant remains to be seen.

*All authors contributed to the writing and conception of the manuscript. The authors also declare that they have no potential conflicts of interest.*

*Manuscript received April 12, 2005. Accepted August 30, 2005.*

## References

- Davie EW, Ratnoff OD. Waterfall Sequence for intrinsic blood clotting. *science* 1964;145:1310-2.
- Macfarlane RG. An enzyme cascade in the blood clotting mechanism, and its function as a biochemical amplifier. *Nature* 1964;202:498-9.
- Rost S, Fregin A, Ivaskevicius V, Conzelmann E, Hortnagel K, Pelz HJ, et al. Mutations in VKORC1 cause warfarin resistance and multiple coagulation factor deficiency type 2. *Nature* 2004;427: 537-41.
- Bevers EM, Rosing J, Zwaal RF. Development of procoagulant binding sites on the platelet surface. *Adv Exp Med Biol* 1985;192:359-71.
- Tuddenham EG. Blood coagulation proceeds and is terminated by successive formation of macromolecular complexes. Educational book, 5th Congress of the European Haematology Association. 2000. p. 178-80.
- Berman HM, Westbrook J, Feng Z, Gilliland G, Bhat TN, Weissig H, et al. The Protein Data Bank. *Nucleic Acids Res* 2000;28:235-42.
- van't Veer C, Mann KG. Regulation of tissue factor initiated thrombin generation by the stoichiometric inhibitors tissue factor pathway inhibitor, antithrombin-III, and heparin cofactor-II. *J Biol Chem* 1997; 272:4367-77.
- Broze GJ Jr. Tissue factor pathway inhibitor. *Thromb Haemost* 1995;74: 90-3.
- Baugh RJ, Broze GJ Jr, Krishnaswamy S. Regulation of extrinsic pathway factor Xa formation by tissue factor pathway inhibitor. *J Biol Chem* 1998;273: 4378-86.
- Hansen JB, Huseby NE, Sandset PM, Svensson B, Lyngmo V, Nordoy A. Tissue-factor pathway inhibitor and lipoproteins. Evidence for association with and regulation by LDL in human plasma. *Arterioscler Thromb* 1994;14: 223-9.
- Brodin E, Svensson B, Paulssen RH, Nordoy A, Hansen JB. Intravascular release and urinary excretion of tissue factor pathway inhibitor during heparin treatment. *J Lab Clin Med* 2004;144:246-53.
- Hamik A, Setiadi H, Bu G, McEver RP, Morrissey JH. Down-regulation of monocyte tissue factor mediated by tissue factor pathway inhibitor and the low density lipoprotein receptor-related protein. *J Biol Chem* 1999;274:4962-9.
- Sevinsky JR, Rao LV, Ruf W. Ligand-induced protease receptor translocation into caveolae: a mechanism for regulating cell surface proteolysis of the tissue factor-dependent coagulation pathway. *J Cell Biol* 1996;133:293-304.
- Ho G, Toomey JR, Broze GJ Jr, Schwartz AL. Receptor-mediated endocytosis of coagulation factor Xa requires cell surface-bound tissue factor pathway inhibitor. *J Biol Chem* 1996; 271:9497-502.
- Rao LV, Pendurthi UR. Regulation of tissue factor-factor VIIa expression on cell surfaces: a role for tissue factor-factor VIIa endocytosis. *Mol Cell Biochem* 2003; 253:131-40.
- Ahamed J, Belting M, Ruf W. Regulation of tissue factor-induced signaling by endogenous and recombinant tissue factor pathway inhibitor 1. *Blood* 2005; 105:2384-91.
- Piro O, Broze GJ Jr. Role for the Kunitz-3 domain of tissue factor pathway inhibitor-a in cell surface binding. *Circulation* 2004;110:3567-72.
- Bajaj MS, Birktoft JJ, Steer SA, Bajaj SP. Structure and biology of tissue factor pathway inhibitor. *Thromb Haemost* 2001;86:959-72.
- Chand HS, Schmidt AE, Bajaj SP, Kisiel W. Structure-function analysis of the reactive site in the first Kunitz-type domain of human tissue factor pathway inhibitor-2. *J Biol Chem* 2004;279: 17500-7.
- Mann KG, Brummel K, Butenas S. What is all that thrombin for? *J Thromb Haemost* 2003;1:1504-14.
- Huntington JA. Mechanisms of glycosaminoglycan activation of the serpins in hemostasis. *J Thromb Haemost* 2003; 1:1535-49.
- Huntington JA, Read RJ, Carrell RW. Structure of a serpin-protease complex shows inhibition by deformation. *Nature* 2000;407:923-6.
- Stubbs MT, Bode W. The clot thickens: clues provided by thrombin structure. *Trends Biochem Sci* 1995;20:23-8.
- Dementiev A, Petitou M, Herbert JM, Gettins PG. The ternary complex of antithrombin-anhydrothrombin-heparin reveals the basis of inhibitor specificity. *Nat Struct Mol Biol* 2004; 11:863-7.
- Sheehan JP, Sadler JE. Molecular mapping of the heparin-binding exosite of thrombin. *Proc Natl Acad Sci USA* 1994; 91:5518-22.
- Esmon CT. Regulation of blood coagulation. *Biochim Biophys Acta* 2000; 1477:349-60.
- Esmon CT. Thrombomodulin as a model of molecular mechanisms that modulate protease specificity and function at the vessel surface. *FASEB J* 1995;9:946-55.
- Fuentes-Prior P, Iwanaga Y, Huber R, Pagila R, Rumennik G, Seto M, et al. Structural basis for the anticoagulant activity of the thrombin-thrombomodulin complex. *Nature* 2000;404:518-25.
- He X, Ye J, Esmon CT, Rezaie AR. Influence of arginines 93, 97, and 101 of thrombin to its functional specificity. *Biochemistry* 1997;36:8969-76.
- Dahlback B, Villoutreix BO. The anticoagulant protein C pathway. *FEBS Lett* 2005; 579:3310-6.
- Hurtado V, Montes R, Gris JC, Bertolaccini ML, Alonso A, Martinez-Gonzalez MA, et al. Autoantibodies against EPCR are found in antiphospholipid syndrome and are a risk factor for fetal death. *Blood* 2004;104:1369-74.
- Sun YH, Shen L, Dahlback B. Gla domain-mutated human protein C exhibiting enhanced anticoagulant activity and increased phospholipid binding. *Blood* 2003;101:2277-84.
- Esmon CT. Inflammation and thrombosis. *J Thromb Haemost* 2003;1:1343-8.
- Van de Wouwer M, Conway EM. Thrombomodulin: a regulator of coagulation, fibrinolysis, inflammation and cell proliferation. In: Arnout J, de Gaetano G, Hoylaerts MF, Peerlinck K, Van Geet C, Verhaeghe R, editors. *Thrombosis: Fundamental and Clinical Aspects*. Leuven University Press, 2003. p. 225-40.
- Rezende SM, Simmonds RE, Lane DA. Coagulation, inflammation, and apoptosis: different roles for protein S and the protein S-C4b binding protein complex. *Blood* 2004;103:1192-201.

**Effects of the protein tyrosine kinase inhibitor, SU5614, on leukemic and normal stem cells**

**FLT3 activating mutations are the most frequent single genetic abnormality in patients with acute myeloid leukemia. Thus targeting the FLT3 activated kinase is a promising treatment approach. We wanted to test whether the protein tyrosine kinase inhibitor SU5614 selectively eliminates leukemic stem cells while sparing their normal counterparts.**

haematologica 2005; 90:1577-1578  
(<http://www.haematologica.org/journal/2005/11/1577.html>)

The most common single genetic alterations in acute myeloid leukemia (AML) are activating mutations of *FLT3* such as the internal tandem duplication (*FLT3-LM*) or mutations in the second tyrosine kinase domain at codons 835, 836, 841, or 842 (*FLT3-TKD*).<sup>1</sup> These mutations constitutively activate protein tyrosine kinases, inducing factor-independent growth of hematopoietic cell lines or a myeloproliferative syndrome in mice.<sup>2,3</sup> Recently, a number of small molecule protein tyrosine kinase inhibitors have been developed which target constitutively activated FLT3. One member of the family of protein tyrosine kinase inhibitors is SU5614, which suppresses growth factor-independent growth of cells with constitutively activated FLT3 *in vitro* and has anti-leukemic activity in patients with AML or myelodysplastic syndrome.<sup>4-6</sup> However, like other protein tyrosine kinase inhibitors, SU5614 does not inhibit FLT3 selectively, but also inhibits stem cell factor receptor and vascular endothelial growth factor receptor. Activity against several protein tyrosine kinases has the advantage that the anti-leukemic potential of compounds such as SU5614

might not be restricted to FLT3-LM or FLT3-TKD, as demonstrated in the first clinical trials.<sup>4,5</sup> However, both receptors are pivotal for normal hematopoietic stem cell (HSC) development<sup>7</sup> and, therefore, might result in substantial toxicity against normal HSC. The aim of this study was to analyze and compare the effects of SU5614 on AML HSC and normal HSC.

Peripheral blood or bone marrow cells were obtained from 12 patients with newly-diagnosed AML after informed consent and with the approval of the Clinical Research Ethics Board of the LMU University of Munich. The diagnosis and classification of AML were based on the criteria of the French-American-British (FAB) group.<sup>8</sup> Cytogenetic analysis was performed on the bone marrow at initial diagnosis. Frozen normal CD34<sup>+</sup> bone marrow cells were obtained from CellSystems (St. Katharinen, Germany). Analysis of FLT3-TKD and FLT3-LM was performed as described previously.<sup>1,9</sup> AML bone marrow or peripheral blood as well as CD34<sup>+</sup> bone marrow cells from healthy donors were incubated at 1×10<sup>6</sup> cells/mL with 50 ng/mL granulocyte colony-stimulating factor with or without (control) 10 μmol SU5614 (Calbiochem-Novabiochem, Bad Soden, Germany). This concentration was previously found to induce apoptosis in transduced myeloid leukemic cell lines.<sup>6</sup> After 24h incubation, equal fractions of the cells recovered from cultures with or without SU5614 were assayed without regard to change in cell numbers. Assays for colony-forming cells (CFC) for AML and normal bone marrow samples were performed as described previously,<sup>10</sup> plating 1-2×10<sup>5</sup> cells/mL in methylcellulose medium (CellSystems). Cultures were scored for the presence of clusters and colonies after 14 days.<sup>10</sup> Long-term culture-initiating cells (LTC-IC) were established from AML and normal bone marrow as previously described.<sup>10</sup> All experiments were done in triplicates. The mean values were used for our analyses. Statistical analysis comprised a Student's t-test (Microsoft

**Table 1.** Patients' characteristics and response to treatment.

Patient	Cytogenetics	Age	FAB	WBC (x10 <sup>9</sup> )	% blasts	FLT3	% killing CFC	LTC-IC
1	46,XX, Nras+	68	M1	284	95	WT	0	100
2	47,XX,I(21),+i(21), c-KIT-, Nras-	67	M2	41	60	WT	0	100
3	46,XY, c-KIT-, Nras-	46	M4	105	90	WT	93	25
4	47,XY,+13, 48,XY,+13,+13, c-KIT-	71	M1	160	90	WT	26	59
5	46,XY, c-KIT-, MLL dupl-	47	M1	66.4		LM	98	100
6	46,XX, Nras-	55	M4	8.2	90	LM	77	100
7	46,XX, c-KIT-	73	M5b	206	90	LM	77	0
8	46,XX,t(11;16), c-KIT-, Nras-	42	M4	75	90	LM	n.g.	69
9	47,XX,+14, c-KIT-, Nras-	68	M5a	94	95	D835H	32	0
10	46,XX, c-KIT-, Nras-	85	M5b	268	95	D835H	100	100
11	46,XY, c-KIT-, Nras-	48	M2	9	80	Del835	n.g.	83
12	46,XX, c-KIT-, Nras-	38	M4	10,6	90	D835Y/ITD	n.g.	14

n.s. not successful; n.g. no growth in control arm; WT: wild type; % killing as compared to AML or normal BM CFC and LTC-IC respectively, after 24 hrs pre-incubation without SU5614 (control).



Excel).

Three groups of patients (n=4 per group) were analyzed with non-mutated wild-type FLT3, FLT3-LM, and FLT3-TKD (D835H, D835Y, del835). The *in vitro* results from each group treated with SU5614 were compared to those of the respective untreated control cells. At the level of clonogenic progenitors (CFC) 2/4 patients with wild-type FLT3, 3/3 with FLT3-LM ( $p < 0.004$ ) and 2/2 with FLT3-TKD responded to therapy with as much as 100% reduction of the number of leukemic CFC as compared to the untreated AML cells (Table 1). At the level of HSC (LTC-IC), the compound achieved > 50% cell killing in 3/4 ( $p < 0.03$ ) patients with wild-type FLT3, 3/4 with FLT3-LM ( $p < 0.04$ ) and 2/4 with FLT3-TKD. The response of both CFC as well as leukemic HSC to SU5614 could not be predicted from the level of expression of FLT3 or the presence of activating mutations or surface expression of c-KIT, a protein tyrosine kinase also targeted by the SU5614 compound (*data not shown*). As a control, CD34<sup>+</sup> bone marrow stem cells from healthy donors were analyzed in the same way. At the level of CFC level SU5614 had considerable toxicity, killing a mean (range) of 67.5 % (30-100) of the cells (n=3). In addition, the compound eliminated normal HSC (n=3) with a range between 78 – 100% after 24h incubation. These data demonstrate the efficacy of tyrosine kinase inhibitors at eliminating leukemic stem cells in AML patients with mutated as well as non-mutated FLT3. However, the data also point to a considerable toxicity to normal HSC, which should be taken into account in the management of patients with compromised normal hematopoiesis.

Natalia Arseni,\*<sup>o</sup> Farid Ahmed,\*<sup>o</sup> Wolfgang Hiddemann,\*<sup>o</sup>  
Christian Buske,\*<sup>o</sup> Michaela Feuring-Buske\*<sup>o</sup>

\*GSF, Clinical Cooperative Group Leukemia Grosshadern,  
Munich, Germany; <sup>o</sup>Department of Medicine III,  
Ludwigs-Maximilian University, Munich, Germany

Funding: this work was supported by a grant from the Deutsche  
Krebshilfe, Bonn, Germany (70-2968 to M.F.-B).

Acknowledgments: we thank B. Ksienzyk for excellent  
technical assistance, K. Spiekermann for providing the SU5614  
compound and C. Schoch, S. Schnittger and W. Kern for  
contributing cytogenetic, molecular and immunophenotypic analyses.

Key words: AML, FLT-3, leukemic stem cell, receptor tyrosine  
kinase inhibitor

Correspondence: Dr. Michaela Feuring-Buske, Department of  
Medicine III, Klinikum Grosshadern, Marchioninstrasse 15,  
81377 Munich, Germany. Phone: international +49.89.7099425.  
Fax: international +49.89.7099400. E-mail: feuring@gsf.de

## References

1. Schnittger S, Schoch C, Dugas M, Kern W, Staib P, Wuchter C, et al. Analysis of FLT3 length mutations in 1003 patients with acute myeloid leukemia: correlation to cytogenetics, FAB subtype, and prognosis in the AMLCG study and usefulness as a marker for the detection of minimal residual disease. *Blood* 2002;100:59-66.
2. Kelly LM, Liu Q, Kutok JL, Williams IR, Boulton CL, Gilliland DG. FLT3 internal tandem duplication mutations associated with human acute myeloid leukemias induce myeloproliferative disease in a murine bone marrow transplant model. *Blood* 2002;99:310-8.
3. Spiekermann K, Pau M, Schwab R, Schmieja K, Franzrahe S, Hiddemann W. Constitutive activation of STAT3 and STAT5 is induced by leukemic fusion proteins with protein tyrosine kinase activity and is sufficient for transformation of hematopoietic precursor cells. *Exp Hematol* 2002;30:262-71.
4. Fiedler W, Mesters R, Tinnefeld H, Loges S, Staib P, Duhrsen U, et al. A phase 2 clinical study of SU5416 in patients with refractory acute myeloid leukemia. *Blood* 2003;102:2763-7.
5. Giles FJ, Stopeck AT, Silverman LR, Lancet JE, Cooper MA, Hannah AL, et al. SU5416, a small molecule tyrosine kinase receptor inhibitor, has biologic activity in patients with refractory acute myeloid leukemia or myelodysplastic syndromes. *Blood* 2003;102:795-801.
6. Spiekermann K, Dirschinger RJ, Schwab R, Bagrintseva K, Faber F, Buske C, et al. The protein tyrosine kinase inhibitor SU5614 inhibits FLT3 and induces growth arrest and apoptosis in AML-derived cell lines expressing a constitutively activated FLT3. *Blood* 2003;101:1494-504.
7. Eaves C, Miller C, Cashman J, Conneally E, Petzer A, Zandstra P, et al. Hematopoietic stem cells: inferences from *in vivo* assays. *Stem Cells* 1997;15 Suppl 1:1-5.
8. Bennett JM, Catovsky D, Daniel MT, Flandrin G, Galton DA, Gralnick HR, et al. Proposed revised criteria for the classification of acute myeloid leukemia. A report of the French-American-British Cooperative Group. *Ann Intern Med* 1985; 103:620-5.
9. Yamamoto Y, Kiyoi H, Nakano Y, Suzuki R, Kodera Y, Miyawaki S, et al. Activating mutation of D835 within the activation loop of FLT3 in human hematologic malignancies. *Blood* 2001;97:2434-9.
10. Feuring-Buske M, Frankel AE, Alexander RL, Gerhard B, Hogge DE. A diphtheria toxin-interleukin 3 fusion protein is cytotoxic to primitive acute myeloid leukemia progenitors but spares normal progenitors. *Cancer Res* 2002;62:1730-6.

## Malignant Lymphomas

### Rituximab in patients with mucosal-associated lymphoid tissue-type lymphoma of the ocular adnexa

**Eight patients with ocular adnexal mucosal-associated lymphoid tissue (MALT) lymphoma were treated with rituximab, at diagnosis (n=5) or relapse (n=3). All untreated patients achieved lymphoma regression, while relapsing patients had no benefit. Four responding patients experienced early relapse. The median time to progression was 5 months. The efficacy of rituximab in ocular adnexal lymphoma is lower than that reported for gastric MALT lymphomas.**

haematologica 2005; 90:1578-1580

(<http://www.haematologica.org/journal/2005/11/1578.html>)

Any CD20-positive lymphoproliferative disorder is a potentially suitable candidate for treatment with rituximab. Significant rituximab activity has been reported in extranodal mucosal-associated lymphoid tissue (MALT) lymphomas.<sup>2</sup> However, the clinical activity of this drug in MALT lymphomas arising in different organs remains to be defined.<sup>2</sup> MALT-type ocular adnexal lymphoma is a very indolent malignancy that would appear to be a suitable candidate for treatment with a drug that has an excellent safety profile, such as rituximab. However, the use of rituximab in this setting has been only anecdotally investigated.<sup>1,3-5</sup>

We report a series of eight patients with MALT-type ocular adnexal lymphoma treated with rituximab, at diagnosis (patients #1 to 5) or relapse (patients #6 to 8) (Table 1). Patients were treated with rituximab 375 mg/m<sup>2</sup>, weekly, for four weeks, according to the conventional administration schedule which includes pre-medication. Patients did not receive steroids or any other concomitant antineoplastic therapy. CD20-positivity and MALT lymphoma histotype were confirmed both at diagnosis and relapse in all

cases. All patients had measurable disease in the ocular adnexa, and two had concomitant systemic disease (Table 1). The study conformed to the tenets of the Declaration of Helsinki.

The tolerance to rituximab was excellent. All five patients treated at diagnosis (patients #1 to 5) had an objective response, which was complete in three cases and partial in two (Table 1); however, four of them experienced local relapse and one of these four also had a systemic relapse. Patients treated with rituximab for relapsed lymphoma (patients #6 to 8) did not achieve an objective response. After a median follow-up from rituximab administration of 46 months, treatment had failed in all patients but one (patient #4), with a median time to progression for the entire series of 5 months. All patients are alive at a median follow-up of 62 months.

This is the largest reported experience on patients with MALT-type ocular adnexal lymphoma treated with rituximab as a single agent. This drug has been associated with modest activity in advanced MALT lymphomas,<sup>5</sup> but with a 73% response rate in a phase II trial on different extranodal MALT lymphomas.<sup>1</sup> Consistently with our observations, reported response rates have been significantly higher among previously untreated patients than among relapsing patients. The activity of rituximab has been reported to be similar in gastric and non-gastric MALT lymphomas;<sup>1</sup> however, an analysis according to extranodal site has not been provided, and the median follow-up was 15 months, thus preventing any conclusion being drawn about long-term results.

To date, only one paper focusing on the activity of rituximab in ocular adnexal lymphoma is available.<sup>3</sup> This study included two patients with conjunctival MALT lymphoma that had relapsed after radiotherapy in whom rituximab then achieved durable remissions. The only patient in our series who did not experience relapse after rituximab had a conjunctival lymphoma. In another study,<sup>4</sup> the role of rituximab was investigated in eight patients with ocular adnexal lymphoma of different histotypes, including three patients with MALT lymphoma. In that study,<sup>4</sup> rituximab was used in combination with chemotherapy and/or radiotherapy, thus preventing any conclusion being drawn about the real efficacy of the monoclonal antibody. Consistently with our observations, however, two of the three patients with MALT lymphoma experienced early relapse after rituximab-containing therapy. Anecdotally, rituximab activity has been reported in a few cases of ocular adnexal lymphoma other than of MALT-type; stage, management and follow-up were variable.<sup>4,7,8</sup>

Our experience suggests a discrepancy between the activity and efficacy of rituximab against MALT lymphomas arising in the ocular adnexa and those occurring in the stomach. In fact, despite a high activity in both lymphomas, the efficacy of rituximab against ocular adnexal lymphoma of MALT-type seems to be lower than that reported for gastric MALT lymphoma.<sup>9</sup> In a retrospective series of 26 patients with gastric MALT lymphoma, 77% of the patients responded to rituximab and only two patients had relapses, after a median follow-up of 33 months.<sup>9</sup> These results clearly contrast with the treatment failures observed in seven of our eight patients and the median time to progression of 5 months. These differences in the efficacy of rituximab could be in part explained by the known heterogeneity of extranodal MALT lymphomas, which display a different natural behavior according to the organ in which they arise.<sup>2</sup>

**Table 1.** Stage, extent of disease, objective response, and duration of response after rituximab.

N.	Sex/ Age	Stage disease	Orbital disease	Systemic	Therapy line <sup>f</sup>	Objective response* (mo.)	TTP (mo.)	Site of relapse
1	F/56	IV	lacrimal gland	stomach, mediastinum & axillary lymph n.	1 <sup>st</sup>	CR	23	L
2	F/59	IV	lacrimal gland (bilateral)	—	1 <sup>st</sup>	CR	17	L
3	F/74	I	orbit	—	1 <sup>st</sup>	PR	48	L + S <sup>§</sup>
4	F/38	I	conjunctiva	—	1 <sup>st</sup>	CR	37+	
5	F/48	I	conjunctiva	—	1 <sup>st</sup>	PR	2	L
6	F/22	I	orbit	—	2 <sup>nd</sup>	PD	0	L
7	F/74	IV	orbit	bone marrow, parotid gland & cervical lymph n.	3 <sup>rd</sup>	PD	0	L
8	M/55	IV	conjunctiva (bilateral)	—	5 <sup>th</sup>	SD	5	L

No patient had ECOG-PS >1, systemic symptoms or elevated levels of serum lactate dehydrogenase. <sup>a</sup>Patient #6 had been previously treated with CEOP chemotherapy, patient #7 with CEOP chemotherapy and orbital irradiation, and patient #8 with orbital irradiation, CHOP chemotherapy, doxycycline, and intralesional interferon. <sup>b</sup>Objective response was defined according to the WHO criteria. <sup>c</sup>CR: complete remission; PR: partial response; PD: progressive disease; SD: stable disease; TTP: the time to progression was calculated from therapy conclusion to the date of lymphoma progression or last date of follow-up; <sup>d</sup>“+” indicates the absence of lymphoma progression after therapy. L: local; S: systemic. Preliminary data concerning patients #1 and 2 have been previously reported. <sup>e</sup>Systemic relapse consisted of lymphomatous involvement of axillary lymph nodes and subcutaneous nodules.

In conclusion, rituximab is highly active against newly diagnosed ocular adnexal lymphoma, while it is inefficient in relapsing patients. Its activity is similar to that observed in other extranodal MALT lymphomas, but its long-term efficacy is modest. The relapse rate in patients with ocular adnexal MALT lymphoma is clearly higher than that reported for gastric MALT lymphoma, suggesting that MALT lymphomas arising in different organs could show varied sensitivity to rituximab. Further investigations will be needed to define the best role for rituximab in the management of extranodal MALT lymphomas.

Andrés J.M. Ferreri,<sup>\*</sup> Maurilio Ponzoni,<sup>°</sup> Giovanni Martinelli,<sup>#</sup>  
Giuliana Muti,<sup>¶</sup> Massimo Guidoboni,<sup>^</sup> Riccardo Dolcetti,<sup>^</sup>  
Claudio Dogliani<sup>°</sup>

Medical Oncology Unit<sup>\*</sup> and Pathology Unit,  
<sup>°</sup>San Raffaele H Scientific Institute, Milan, Italy;

<sup>#</sup>Division of Hematology, European Institute of Oncology, Milan;

<sup>¶</sup>Division of Hematology, IRCCS Niguarda Cà Granda, Milan;

<sup>^</sup>Immunovirology and Biotherapy Unit, Dept. of Pre-Clinical  
and Epidemiological Research, Centro di Riferimento Oncologico,  
IRCCS National Cancer Institute, Aviano, Italy

Key words: MALT lymphoma, ocular adnexal lymphoma,  
rituximab.

Correspondence: Andrés J.M. Ferreri, MD, Medical Oncology  
Unit, Dept. of Oncology, San Raffaele H Scientific Institute,  
Via Olgettina 60, 20132, Milan, Italy. Phone: international  
+39.02.26437649. Fax: international +39.02.26437603.  
E-mail: andres.ferreri@hsr.it

## References

1. Conconi A, Martinelli G, Thieblemont C, Ferreri AJ, Devizzi L, Peccatori F, et al. Clinical activity of rituximab in extranodal marginal zone B-cell lymphoma of MALT type. *Blood* 2003;102:2741-5.
2. Zucca E, Conconi A, Pedrinis E, Cortelazzo S, Motta T, Gospodarowicz MK, et al. Nongastric marginal zone B-cell lymphoma of mucosa-associated lymphoid tissue. International Extranodal Lymphoma Study Group. *Blood* 2003;101:2489-95.
3. Nuckel H, Meller D, Steuhl KP, Duhrsen U. Anti-CD20 monoclonal antibody therapy in relapsed MALT lymphoma of the conjunctiva. *Eur J Haematol* 2004;73:258-62.
4. Sullivan TJ, Grimes D, Bunce I. Monoclonal antibody treatment of orbital lymphoma. *Ophthalm Plast Reconstr Surg* 2004;20:103-6.
5. Raderer M, Jager G, Brugger S, Puspok A, Fiebiger W, Drach J, et al. Rituximab for treatment of advanced extranodal margin-

al zone B cell lymphoma of the mucosa-associated lymphoid tissue lymphoma. *Oncology* 2003;65:306-10.

6. Zubrod CG, Scheidermann MA, Frei E. Appraisal of methods for the study of chemotherapy in man: comparative therapeutic trial of nitrogen mustard and triethylene thiophosphoramide. *J Chronic Dis* 1960;11:7-33.
7. Zinzani PL, Alinari L, Stefoni V, Loffredo A, Pichierri P, Polito E. Rituximab in primary conjunctiva lymphoma. *Leuk Res* 2005;29:107-8.
8. Esmaeli B, Murray JL, Ahmadi MA, Naderi A, Singh S, Romaguera J, et al. Immunotherapy for low-grade non-hodgkin secondary lymphoma of the orbit. *Arch Ophthalmol* 2002;120:1225-7.
9. Martinelli G, Laszlo D, Ferreri AJ, Pruneri G, Ponzoni M, Conconi A, et al. Clinical activity of rituximab in gastric marginal zone non-Hodgkin's lymphoma resistant to or not eligible for anti-Helicobacter pylori therapy. *J Clin Oncol* 2005;23:1979-83.

## Malignant Lymphomas

## High-dose therapy with autologous stem cell transplantation in first response in mantle cell lymphoma

**We retrospectively investigated the outcome of 30 newly diagnosed patients with mantle cell lymphoma treated with high-dose therapy and autologous stem cell transplantation in first response. With a median follow-up of 55 months, the 5-year overall-survival is 62%, the 5-year progression-free-survival is 40% and no secondary malignancy has occurred.**

*haematologica* 2005; 90:1580-1582

(<http://www.haematologica.org/journal/2005/11/1580.html>)

We performed a retrospective analysis of patients under 65 years of age diagnosed with mantle cell lymphoma (MCL) in our department between 1990 and 2003. Our therapeutic strategy for these patients always included autologous stem cell transplantation (ASCT) in first response. Thirty-five patients were diagnosed as having MCL in this period. However, five patients were excluded from the study: one because he received an allogeneic stem cell transplantation and four because they had progressive disease after initial chemotherapy.

The induction therapy consisted of three to four courses of increased CHOP-like or CHOP regimen. The DHAP or an ESHAP regimen was used to obtain a response before ASCT in patients with stable disease following the CHOP or CHOP-like regimen. Response was assessed by physical examination, hemogram and blood chemistry analysis, chest X-ray, thoracic, abdominal and pelvic computed tomography, and bone marrow biopsy if positive at diagnosis. The response was evaluated after the initial chemotherapy, 3 months after ASCT, twice a year for 5 years, and then yearly up to 10 years. Complete response was defined as the complete disappearance of lymphoma. Regression of at least 50% of all measurable disease was defined as a partial response. Minimal response and stable disease were defined as reductions of all measurable lesions of, respectively, 25% to 50% and 0% to 25%.

The patients' initial characteristics are listed in Table 1A and the characteristics of their transplants are summarized in Table 1B. The median follow-up is 55 months (range: 13-149 months). As shown in Figure 1A, the 5-year overall

Table 1A. Initial patient characteristics.

	n (%)
<b>Age (years)</b>	
Median	53
Range	40-63
<b>International Prognostic Index</b>	
Low-risk	10 (33)
Low-intermediate risk	13 (43)
High-intermediate risk	4 (14)
High-risk	2 (7)
Unknown	1 (3)
<b>Sex</b>	
Male	23 (77)
Female	7 (23)
<b>Ann Arbor stage</b>	
III	4 (14)
IV	26 (86)
<b>B symptoms</b>	
Present	8 (27)
Absent	19 (63)
Unknown	3 (10)
<b>Performance status</b>	
<2	30 (100)
≥2	0 (0)
<b>Lactate dehydrogenases</b>	
Normal level	17 (57)
Above normal	12 (40)
Unknown	1 (3)
<b>Dimension of the largest tumor mass</b>	
≥10 cm	5 (17)
<10 cm	23 (77)
Unknown	2 (6)
<b>Site of extra-nodal disease</b>	
Bone marrow	23 (77)
Blood	15 (50)
Gastrointestinal tract	11 (37)
Liver	7 (23)
Lung	1 (3)
<b>Extranodal sites</b>	
0	4 (13)
1	14 (47)
2	6 (20)
3	6 (20)

**Table 1B.** Characteristics at transplantation.

	n (%)
<b>Time from diagnosis to transplantation</b>	
Median	5 months
<b>Source of stem cells</b>	
Peripheral blood	27 (90)
Bone marrow	3 (10)
<b>Conditioning regimen</b>	
TBI+Cy	23 (77)
BEAM	5 (17)
TBI+CBV	1 (3)
TBI+Mel	1 (3)
<b>Post-transplant growth factors</b>	
G-CSF	22 (72)
GM-CSF	4 (14)
None	4 (14)
<b>Number of chemotherapy lines before transplantation</b>	
1	23 (77)
2	6 (20)
3	1 (3)
<b>Status at transplantation</b>	
Complete response	5 (17)
Partial response	24 (80)
Minimal response	1 (3)
<b>Response 90 days after transplant</b>	
Complete response	26 (87)
Partial response	3 (10)
Progressive disease	1 (3)

TBI+Cy: total body irradiation of 12 Gy in 6 fractions over 3 days plus cyclophosphamide (60 mg/kg/day for 2 consecutive days); BEAM: BCNU: 300 mg/m<sup>2</sup> day 1; etoposide: 200 mg/m<sup>2</sup> days 2-5; aracytine: 400 mg/m<sup>2</sup> days 2-5 and melphalan: 140 mg/m<sup>2</sup> day 6; CBV: cyclophosphamide: 1500 mg/m<sup>2</sup> days 1-4; BCNU: 300 mg/m<sup>2</sup> day 1 and etoposide: 200 mg/m<sup>2</sup> days 2-4; Mel: melphalan 140 mg/m<sup>2</sup>.

**Table 2.** Extra-hematological toxicity of ASCT.

	n
Toxic death	0
Secondary malignancy	0
Herpes zoster infection	4
Localized basal cell skin carcinoma	2

survival is 62% and the median overall survival is 72 months. Thirteen patients have died at a median time of 34 months (range: 6-75 months): 11 from lymphoma and 2 from bacterial sepsis. As shown in Figure 1B, the 5-year progression free survival is 40% and the median progression-free survival is 37 months. Seventeen patients have relapsed or progressed at a median time of 22 months (range: 3-111 months). Among these, 13 relapsed from a complete remission at a median time of 22 months (range: 7-111 months). These 13 patients were treated with conventional chemotherapy (n=9) or allogeneic stem cell transplantation (n=4). Three patients in partial remission

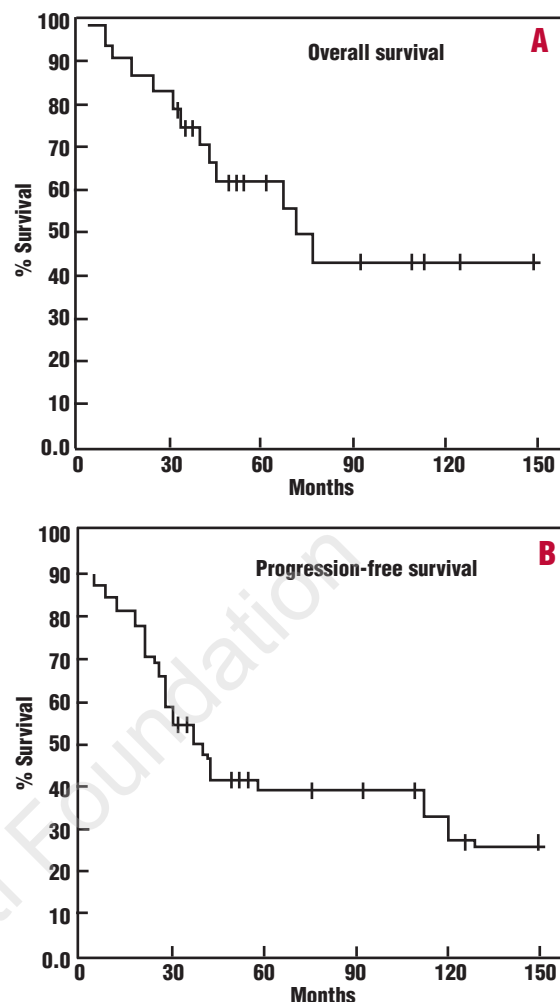


**Figure 1.** A. Overall survival of the studied population. B. Progression-free survival of the studied population.

after ASCT progressed at 4, 10 and 26 months and were treated with conventional chemotherapy. One patient progressed immediately after transplantation and was treated with conventional chemotherapy. Among the 17 relapsing or progressing patients, 13 had died by the time of analysis. High-dose therapy was well tolerated without any toxic deaths during the 3 months following transplantation. The toxicity of the therapy is summarized in Table 2. With a long median follow-up of 55 months, our study shows that patients under 65 years of age responding to initial chemotherapy and subsequently autografted can achieve 5-year progression-free survival and overall survival of, respectively, 40% and 62%, with an acceptable toxicity profile. These results update our previous report on 17 MCL patients who showed 4-year disease-free and overall survivals of, respectively, 49% and 81%.<sup>1</sup> It must be emphasized that 15% of patients (5 out of 35) were not eligible for ASCT because of a poor response to initial chemotherapy. It is also noteworthy that 83% of patients received a conditioning regimen based on total body irradiation and that none developed a secondary malignancy. However, this finding should be viewed cautiously because of the limited size of our study and because a recent prospective study reported an actuarial

risk of 18.6% at 5 years in 86 follicular lymphoma patients autografted in first response.<sup>2</sup> In our study, 23 patients out of 35 (65%) responded to an initial anthracycline-based chemotherapy (CHOP or CHOP-like) while 7 patients needed salvage treatment with high doses of cytarabine before ASCT and 5 patients never obtained a response good enough for ASCT. This proportion of MCL patients responding to an anthracycline-based chemotherapy is consistent with other results reported in the literature.<sup>3</sup> Rituximab is likely to play an important role in association with anthracycline-based chemotherapy by effectively clearing blood and bone marrow lymphoma cells.<sup>4</sup> However, the observation that addition of rituximab to induction therapy does not translate into prolonged progression-free survival supports the role of using ASCT in first response.<sup>5,6</sup>

In a recent landmark study, Dreyling *et al.*<sup>7</sup> demonstrated that ASCT prolongs progression-free survival in MCL. They reported 3-year overall survival and progression-free survival rates of 83% and 54%, respectively. The corresponding 5-year rates in our study, dealing with a comparable population of patients, were 62% and 40%, respectively, thus confirming after an extended follow-up that ASCT in first response is an effective and safe treatment for MCL patients under 65 years of age.

Stéphane Vigouroux,\* Fanny Gaillard,° Philippe Moreau,\*  
Jean-Luc Harousseau,\* Noël Milpied\*

\*Service d'Hématologie Clinique, CHU Hotel Dieu, Nantes,  
France; °Laboratoire d'Anatomie Pathologique,  
CHU Hotel Dieu, Nantes, France

Key words: mantle cell lymphoma, high-dose therapy,  
autologous stem cell transplantation.

Correspondence: Stéphane Vigouroux, MD, Service d'Hématologie  
Clinique, CHU Hotel Dieu, 1 Place Alexis Ricordeau, 44000  
Nantes. Phone: international +33.2.40083271. Fax: international  
+33.2.40083250. E-mail: vigouroux.st@wanadoo.fr

## References

- Milpied N, Gaillard F, Moreau P, Mahe B, Souchet J, Rapp MJ, et al. High-dose therapy with stem cell transplantation for mantle cell lymphoma: results and prognostic factors, a single center experience. *Bone Marrow Transplant* 1998;22:645-50.
- Deconinck E, Foussard C, Milpied N, Bertrand P, Michenet P, Cornillet-LeFebvre P, et al. High-dose therapy followed by autologous purged stem-cell transplantation and doxorubicin-based chemotherapy in patients with advanced follicular lymphoma: a randomized multicenter study by GOELAMS. *Blood* 2005;105:3817-23.
- Oinonen R, Franssila K, Teerenhovi L, Lappalainen K, Elonen E. Mantle cell lymphoma: clinical features, treatment and prognosis of 94 patients. *Eur J Cancer* 1998;34:329-36.
- Gianni AM, Magni M, Martelli M, Di Nicola M, Carlo-Stella C, Pilotti S, et al. Long-term remission in mantle cell lymphoma following high-dose sequential chemotherapy and in vivo rituximab-purged stem cell autografting (R-HDS regimen). *Blood* 2003;102:749-55.
- Howard OM, Gribben JG, Neuberger DS, Grossbard M, Poor C, Janicek MJ, et al. Rituximab and CHOP induction therapy for newly diagnosed mantle-cell lymphoma: molecular complete responses are not predictive of progression-free survival. *J Clin Oncol* 2002;20:1288-94.
- Lenz G, Dreyling M, Hoster E, Wormann B, Duhrsen U, Metzner B, et al. Immunochemotherapy with rituximab and cyclophosphamide, doxorubicin, vincristine, and prednisone significantly improves response and time to treatment failure, but not long-term outcome in patients with previously untreated mantle cell lymphoma: results of a prospective randomized trial of the German Low Grade Lymphoma Study Group (GLSG). *J Clin Oncol* 2005;23:1984-92.
- Dreyling M, Lenz G, Hoster E, Van Hoof A, Gisselbrecht C, Schmits R, et al. Early consolidation by myeloablative radiochemotherapy followed by autologous stem cell transplantation in first remission significantly prolongs progression-free survival in mantle cell lymphoma - results of a prospective randomized trial of the European MCL network. *Blood* 2005; 105:2677-84.

## Stem Cell Transplantation

### Development of functional *Haemophilus Influenzae* type b antibodies after vaccination of autologous stem cell transplant recipients

**Sixteen autologous stem cell transplant recipients received three vaccinations with conjugated *haemophilus influenzae* type b vaccine. Quantitative and qualitative aspects of the antibody response were studied. The vaccination schedule resulted in high antibody response rates and functional maturation of antibodies, as measured by antibody avidity and phagocytosis-inducing capacity.**

haematologica 2005; 90:1582-1584

(<http://www.haematologica.org/journal/2005/11/1582.html>)

Infections are a major source of morbidity in patients undergoing autologous stem cell transplantation and are frequently caused by encapsulated bacteria such as *Haemophilus influenzae* type b (*Hib*) and *Streptococcus pneumoniae*.<sup>1,2</sup> Therefore, vaccination of stem cell transplant recipients with *Hib* and pneumococcal vaccine has been recommended.<sup>3,4</sup> A response to vaccination is often quantitatively expressed as antibody titers, but determination of avidity and phagocytosis-inducing capacity of antibodies can provide important information regarding the functional activity of antibodies.<sup>5,6</sup> For instance, an increase in

antibody avidity during the year following *Hib* vaccination with a concurrent decrease in antibody levels, has been described in children.<sup>7</sup> We conducted a prospective follow-up study to determine quantitative and qualitative aspects of the humoral immune response to multiple vaccinations with conjugated *H. influenzae* type b vaccine in 16 adult patients with non-Hodgkin's lymphoma (n=3) or multiple myeloma (n=13) who underwent autologous stem cell transplantation. Patients with multiple myeloma received high dose melphalan, whereas patients with non-Hodgkin's lymphoma received the BEAM regimen as conditioning therapy. At 6, 8 and 14 months after transplantation, patients were vaccinated with *Hib* (PRP-T vaccine: polyribosylribitolphosphate conjugated to tetanus toxoid). Serum samples were taken before vaccination and 3 weeks after each vaccination. For each patient, sera taken at all time points were analyzed simultaneously for all techniques. IgG antibody levels to *H. influenzae* were measured by ELISA as described previously.<sup>8</sup> An adequate antibody response was defined as a 4-fold or greater increase in antibody levels in addition to a minimal titer of 50 U/mL corresponding to 18.8 µg/mL, which is 50% of the titer in the reference serum. Avidity indices of IgG anti-*Hib* antibodies were measured by a modification of the sodium thiocyanate (NaSCN) elution method described by Pullen *et al.*<sup>9</sup> Antibody avidity can only reliably be determined in sera with a minimal optical density value of 1.0 at a 1:50 dilution, corresponding to a minimal *Hib* antibody concentration of 25 µg/mL. The relative

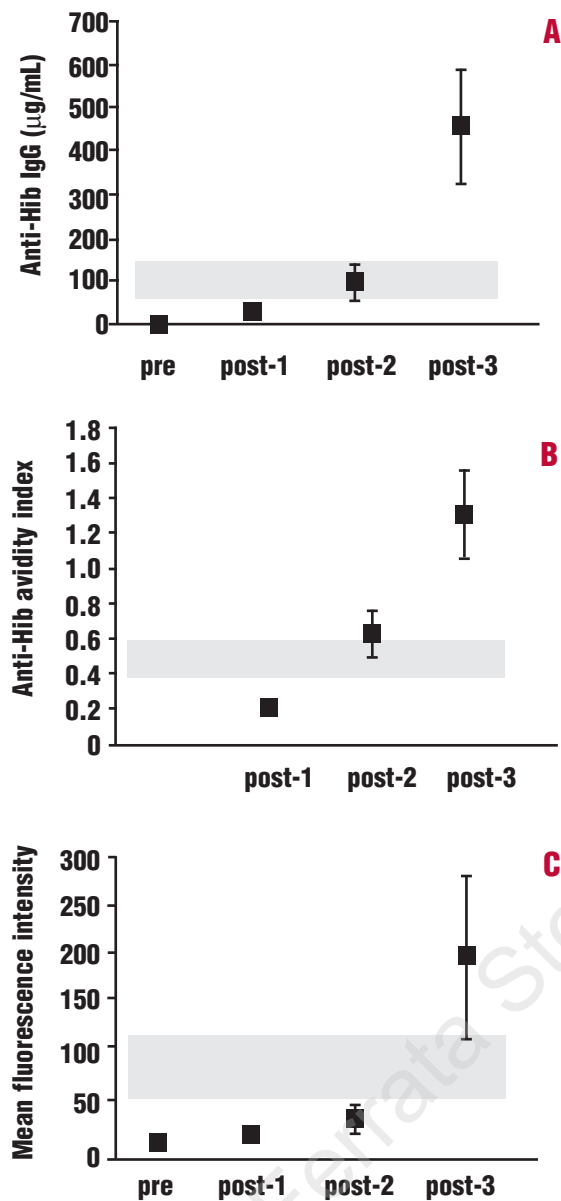


**Figure 1.** A. Anti-*Hib* IgG antibodies of 14 patients before (pre) and after one (post-1), two (post-2) and three (post-3) vaccinations with conjugated *Hib* vaccine. Mean antibody levels plus standard errors are shown. Anti-*Hib* antibodies increased significantly after three vaccinations ( $p$  value=0.001). Hatched area indicates mean value ( $\pm$  SE) of 12 healthy adults vaccinated with a single dose of *Hib* conjugate vaccine. B. Anti-*Hib* IgG antibodies avidity indices (AI) after one (post-1), two (post-2) and three (post-3) vaccinations with *Hib* vaccine. Mean AI plus standard errors are shown. Mean AI increased significantly after three vaccinations with conjugated *Hib* vaccine, as compared with AI after two vaccinations ( $p$  value=0.047). Hatched area indicates mean value ( $\pm$  SE) of 12 healthy adults vaccinated with a single dose of *Hib* conjugate vaccine. C. Phagocytosis inducing capacity of anti-*Hib* IgG antibodies of 14 patients, expressed as mean fluorescence intensity (MFI), before and after one, two and three vaccinations with *Hib* vaccine. MFI plus standard errors are shown. MFI increased significantly after two and three vaccinations, as compared with MFI before vaccination ( $p$  values 0.03 and 0.002, respectively). Hatched area indicates mean value ( $\pm$  SE) of 12 healthy adults vaccinated with a single dose of *Hib* conjugate vaccine.

avidity index (AI) is defined as the molarity of NaSCN at which 50% of the amount of IgG antibodies bound to the coated antigen in the absence of NaSCN has been eluted. Phagocytosis-inducing capacity of anti-*Hib* IgG antibodies was determined by a modification of the method described by Sanders *et al.*<sup>10</sup> In brief, sera of patients were incubated with fluorescein isothiocyanate (FITC)-labeled *Hib*, subsequently incubated with polymorphic mononuclear cells and analyzed by flow cytometry. The phagocytosis-inducing capacity of antibodies was expressed as the mean FITC fluorescence intensity (MFI).

The mean level of CD19<sup>+</sup> cells before vaccination was  $0.17 \times 10^9/L$  (range  $0-0.4 \times 10^9/L$ ) with subnormal levels of B cells in three patients. Two patients had recurrence of tumor at 9 and 12 months after transplantation and were not included in the subsequent analysis. Measurement of antibody titers showed response rates of 38%, 75% and 93% after one, two and three vaccinations, respectively (Figure 1A). One patient did not acquire anti-*Hib* antibodies after any of the three vaccinations. Avidity indices are depicted in Figure 1B. After repeated vaccinations, avidity of anti-*Hib* IgG antibodies increased in all but one of the patients who were eligible for avidity determination. This one patient did show an increase in anti-*Hib* antibodies after all vaccinations, but after the third vaccination the avidity index decreased.

The phagocytosis-inducing capacity of anti-*Hib* IgG antibodies is shown in Figure 1C. The previously mentioned patient who did not acquire anti-*Hib* antibodies did not show an increase in phagocytosis-inducing capacity. This patient had a very low relative CD19-count in the circulation (<1%) at the time of the first vaccination, also reflected by low serum immunoglobulin levels. The patient who had a high increase in antibodies but a decrease in avidity index, also showed a decrease in MFI after the third vaccination. Although this patient did have a robust IgA response after the third *Hib* vaccination (a rise from 163 to 2034 U/mL) which was higher than that in the other patients (range 1 to 643 U/mL after three *Hib* vaccinations), the high IgA antibody response cannot readily explain the drop in IgG avidity, apart from the theoretical possibility that all high affinity IgG-bearing B lymphocytes would have switched to IgA, resulting in blocking of phagocytosis. However, the data do underline the relation between antibody avidity and opsonization/phagocytosis and show that an increase in antibody quantity is not always accompanied by an increase in antibody quality.

In conclusion, in this study of autologous stem cell transplant recipients, multiple vaccinations with a conjugated *Hib* vaccine resulted in high antibody levels and maturation of antibody functionality.

Ankie M.T. van der Velden,<sup>\*\*</sup> Anke M.E. Claessen,<sup>°</sup>  
Heleen van Velzen-Blad,<sup>°</sup> Douwe H. Biesma,<sup>\*</sup> Ger T. Rijkers<sup>#</sup>  
Departments of Internal Medicine\* and Medical Microbiology  
& Immunology,<sup>°</sup> Sint Antonius Hospital Nieuwegein, and  
Department of Immunology, Laboratory of Paediatric Immunology,  
University Children's Hospital "Het Wilhelmina  
Kinderziekenhuis"/University Medical Centre Utrecht,<sup>#</sup>  
the Netherlands

**Key words:** *Haemophilus influenzae* type b, vaccination, autologous stem cell transplantation, phagocytosis.

**Funding:** financially supported by the Dutch Cancer Society.

**Correspondence:** Ankie M.T. van der Velden, Department of Hematology, VU Medical Centre, P.O. Box 7057, 1007 MB, Amsterdam, The Netherlands. Telephone: +31 20 4442604. Fax: +31 20 4442601. E-mail: am.vandervelden@vumc.nl

## References

1. Lossos IS, Breuer R, Or R, Strauss N, Elishoov H, Naparstek E, et al. Bacterial pneumonia in recipients of bone marrow transplantation. A five-year prospective study. *Transplantation* 1995;60:672-8.
2. Frere P, Hermanne JP, Debouge MH, de Mol P, Fillet G, Beguin Y. Bacteremia after hematopoietic stem cell transplantation: incidence and predictive value of surveillance cultures. *Bone Marrow Transplant* 2004;33:745-9.
3. Ljungman P, Engelhard D, de la Camara R, Einsele H, Locasciulli A, Martino R, et al. Vaccination of stem cell transplant recipients: recommendations of the Infectious Diseases Working Party of the EBMT. *Bone Marrow Transplant* 2005;35:737-46.
4. Sullivan KM, Dykewicz CA, Longworth DL, Boeckh M, Baden LR, Rubin R, et al. Preventing opportunistic infections after hematopoietic stem cell transplantation: the Centers for Disease Control and Prevention, Infectious Diseases Society of America, and American Society for Blood and Marrow Transplantation Practice Guidelines and beyond. *Hematology Am Soc Hematol Educ Program* 2001;392-421.
5. Martinez JE, Romero-Steiner S, Pilishvili T, Barnard S, Schinsky J, Goldblatt D, et al. A flow cytometric opsonophagocytic assay for measurement of functional antibodies elicited after vaccination with the 23-valent pneumococcal polysaccharide vaccine. *Clin Diagn Lab Immunol* 1999; 6:581-6.
6. Parkkali T, Kayhty H, Anttila M, Ruutu T, Wuorimaa T, Soininen A, et al. IgG subclasses and avidity of antibodies to polysaccharide antigens in allogeneic BMT recipients after vaccination with pneumococcal polysaccharide and *Haemophilus influenzae* type b conjugate vaccines. *Bone Marrow Transplant* 1999;24:671-8.
7. Goldblatt D, Vaz AR, Miller E. Antibody avidity as a surrogate marker of successful priming by *Haemophilus influenzae* type b conjugate vaccines following infant immunization. *J Infect Dis* 1998;177:1112-5.
8. Breukels MA, Jol-van der Zijde E, van Tol MJ, Rijkers GT. Concentration and avidity of anti-*Haemophilus influenzae* type b (Hib) antibodies in serum samples obtained from patients for whom Hib vaccination failed. *Clin Infect Dis* 2002;34:191-7.
9. Pullen GR, Fitzgerald MG, Hosking CS. Antibody avidity determination by ELISA using thiocyanate elution. *J Immunol Methods* 1986;86:83-7.
10. Sanders LA, Feldman RG, Voorhorst-Ogink MM, de Haas M, Rijkers GT, Capel JA, et al. Human immunoglobulin G (IgG) Fc receptor IIa (CD32) polymorphism and IgG2-mediated bacterial phagocytosis by neutrophils. *Infect Immun* 1995;63:73-81.



Haematologica/The Hematology Journal is associated with USPI Unione Stampa Medica Italiana and receives educational grants from:



IRCCS Policlinico S. Matteo, Pavia, Italy



University of Pavia, Italy